Chapter 8

Symbolic dynamics in special limits

In some limit cases of billiard systems the symbolic dynamics is special and can be found exact. Even if these cases are limits of the alphabets we can derive from a pruning front, the symbolic dynamics of the limit may have very different number theoretical properties than for the typical description. The limit we discuss in this chapter is the integrable limit of the billiards where the orbits are stable and exist in continuous families. The symbolic dynamics is in most cases mapped into a simple rotation which is the description of how a straight line crosses a lattice. The symbolic description of the rotation is a problem with old roots considered by Bernoulli (1772), Markov (1882), Christoffel (1875) and Smith (1877) (for historical notes see ref. [179]). The results as we use it was showed first by Morse and Hedlund [157]. Generalizations to higher dimensions can also be done [18].

Our simplest billiard, the 3 disk system, turns out to be slightly more complicated than the 4 disk billiard and the wedge billiard, so we choose here to first present the method for the later billiards.

In figure 8.1 a square lattice is drawn together with a line crossing the lattice. Denote a crossing of the line with a vertical lattice line 0 and a crossing of the line with a horizontal lattice line 1 . The symbol string $\ldots l_{-2}l_{-1}l_0l_1l_2\ldots$ is the symbolic representation of the different crossings of the line with the lattice lines. The line in figure 8.1 is described by the symbolic string $\ldots 0100100100100010\ldots$. A given infinite symbolic string define uniquely the slope of the line, but a periodic orbit has an interval of starting points giving the same symbolic dynamics. The admissible strings are not constructed from a finite alphabet or from a Markov graph as we have done in other examples, but can be constructed from a Farey tree expansion. The symbolic Farey tree is drawn in figure 8.3.

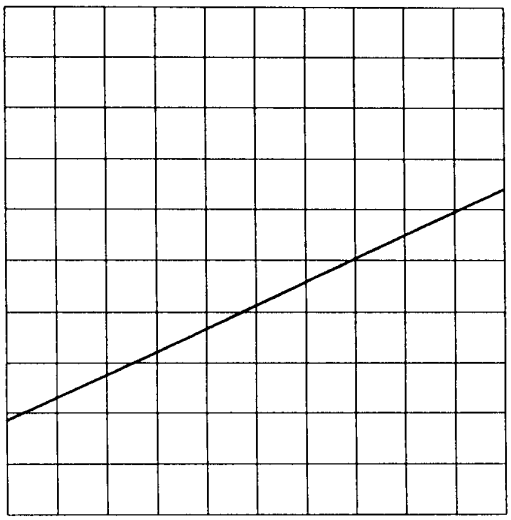

Figure 8.1: The crossing of a straight line with the lines of a square lattice.

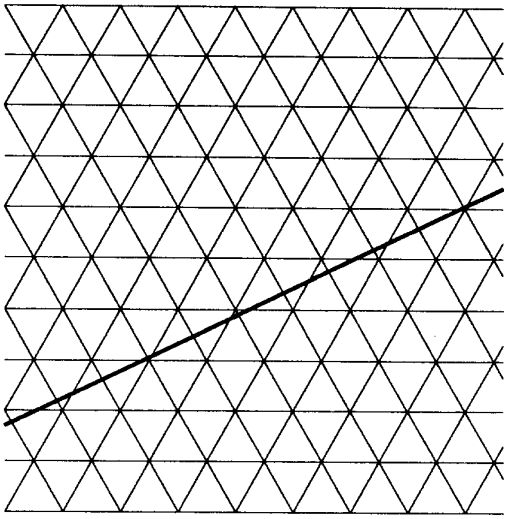

Figure 8.2: The crossing of a straight line with the lines of a triangular lattice.

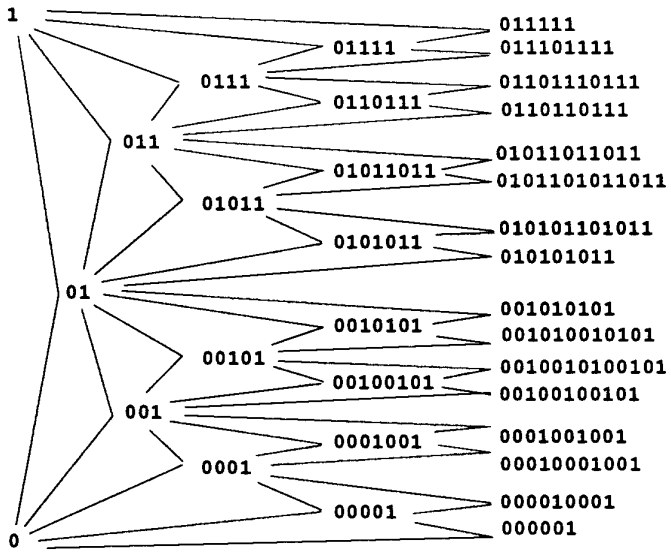

Figure 8.3: The construction of admissible symbolic sequences for the crossings in figure 8.1 by a Farey tree.

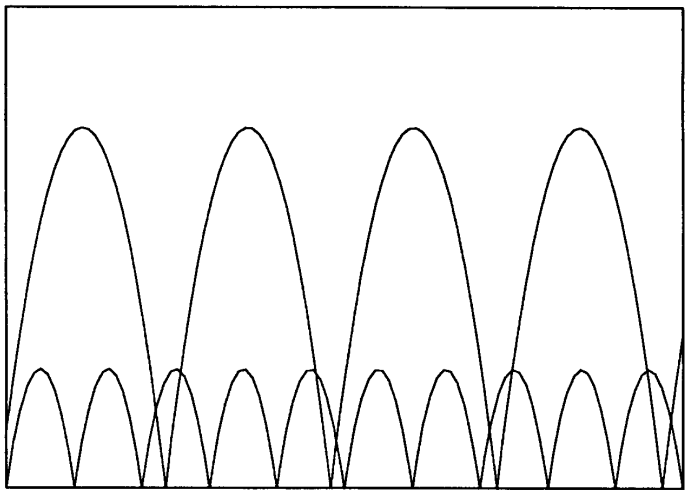

Figure 8.4: Two independent balls bouncing and crossing each others path. The symbolic description of this orbit is ...00110110011011....

To apply this for the billiard examples we have to translate the symbols for vertical and horizontal lines into the symbols in the different billiards.

8.1 Wedge billiard

In the limit where the angle in the wedge billiard goes to 45° the system is integrable and corresponds to a simple rotation. The corresponding system with two bouncing balls is when the two masses are equal $m_1 = m_2$. In this two ball system it is easy to see why a simple rotation is the correct dynamics of the system. An elastic collision between two point particles with equal masses is identical to the system where the two particles pass through each other without any interaction. We then have a crossing of balls instead off bouncing between two balls. If the two balls bounce in the floor independent of each other only the initial position and velocity matters and there are two independent, never changing bouncing patterns. In figure 8.4 two independent bouncing balls are drawn. One ball bounces with a time T_1 between each bounce and the second ball with time $T_2 \geq T_1$. The two times correspond to the vertical and horizontal distances in figure 8.1 and determine the slope of the line. We can associate the crossing of the straight line with a vertical lattice line with the motion where the lower most ball is bouncing twice off the floor without crossing (=bouncing) with the other ball. A symbol 0 in the lattice description corresponds to a symbol 0 in the two ball symbols. The crossing of the straight line with a horizontal line can be related to the sequence from one ball bouncing off

the floor, the two balls cross and the the second ball bounces off the floor, then the balls cross again and the first ball bounces off the floor. This symbol 1 in the lattice symbols corresponds to the symbolic string 11 in the two ball symbols. Figure 8.4 shows that the two ball symbols always appears in pairs.

Interpreted this way the symbols 0 and 1 for crossing vertical and horizontal lines are identical to the symbols 0 and 11 for the two ball system and therefore also the wedge billiard. The strings in figure 8.3 can be translated into the wedge symbols giving the symbols s_t

11				
			011111111	01111111111
		0111111		0111111011111111
			011110111111	011110111111011111111
	01111			01111011110111111
			0110111101111	011011110111101111
		01101111		0110111011011111011
			01101101111	011011011101101111
011				01101101101111
			0011011011	0011011011011
		0011011		00110110011011011
			00110011011	001100110110011011
	0011			001100110011011
			000110011	0001100110011
		00011		00011000110011
			000011	00001100011
0				0000011

(8.1)

This Farey tree is the description of admissible orbits in the integrable wedge in terms of symbolic dynamics. In the well ordered symbols we have to take care of the flipping process but this is simple since all symbol 1 which flip the ordering always come in an even number so the only difference from the symbols above is

that every second symbol 1 is turned into a symbol 0. This gives the symbols w_t

$$
\begin{array}{lllll}
10 & & & & \\
 & & & 010101010 & 01010101010 \\
 & & & & 0101010010101010 \\
 & & 0101010 & & \\
 & & & 010100101010 & 0101001010100101010 \\
 & & & & 010100101001010 \\
 & 01010 & & & \\
 & & & 0100101001010 & 0100101001010010 \\
 & & & & 0100100101001001010 \\
 & & 01001010 & & \\
 & & & 01001001010 & 0100100101001001010 \\
 & & & & 01001001001010 \\
010 & & & & \\
 & & & 0010010010 & 0010010010010 \\
 & & & & 0010010010010010 \\
 & & 0010010 & & \\
 & & & 00100010010 & 0010001001001010 \\
 & & & & 001000100010010 \\
 & 0010 & & & \\
 & & & 000100010 & 0001000100010 \\
 & & & & 00010000100010 \\
 & & 00010 & & \\
 & & & 000010 & 00001000010 \\
 & & & & 0000010 \\
0 & & & &
\end{array}
\tag{8.2}
$$

and the symmetric ones with 0 and 1 interchanged.

We can show that in the symbol plane this gives as the limit of the pruning front the straight line

$$\delta = \frac{1}{2}\gamma + \frac{1}{2} \tag{8.3}$$

Let a line go through one of the crossings between the horizontal and the vertical lattice lines which corresponds to a singular orbit. The line will cross the vertical and the horizontal lattice lines exactly the same way in both directions along the line from the crossing point. The pruning front is given by the symbolic description of all orbits having a double collision between the two balls and the floor simultaneously an this is the point where the vertical and horizontal lattice lines crosses. All points on the pruning front then has the form

$$\ldots l_3 l_2 l_1 l_0' l_0 l_1 l_2 l_3 \ldots$$

The symbol string $l_0' l_0$ describes the crossing of the line with the lattice cross and the string is either 01 or 10. If we choose $l_0' l_0 = 01$ we get the two ball symbol string describing the line

$$\ldots s_5 s_4 s_3 011 s_3 s_4 s_5$$

and the well ordered symbols

$$\ldots w_5 w_4 w_3 010 w_3 w_4 w_5$$

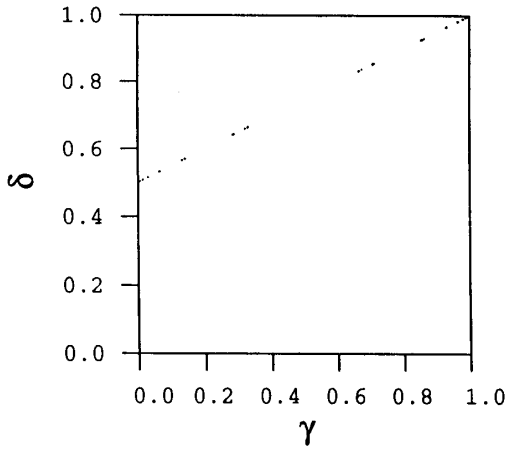

Figure 8.5: The pruning front for the wedge billiard in the integrable case $\theta = 45°$.

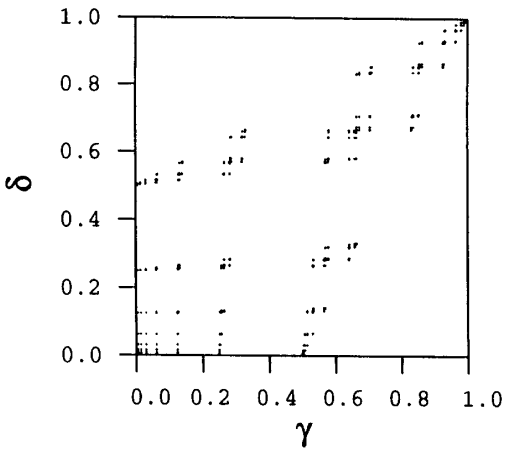

Figure 8.6: The symbolic values for a number of orbits in the wedge billiard in the integrable case $\theta = 45°$.

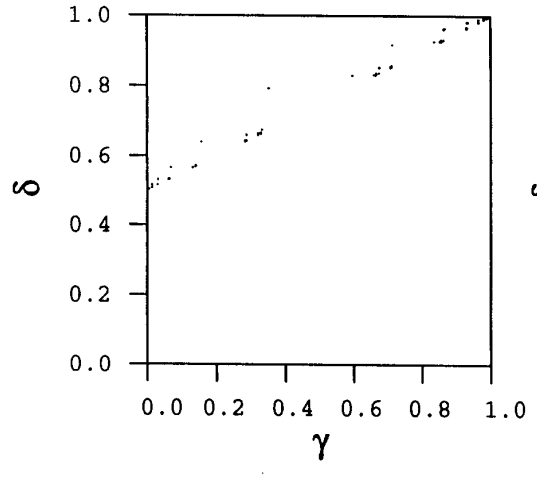

Figure 8.7: The pruning front for the wedge billiard for $\theta = 45.01°$.

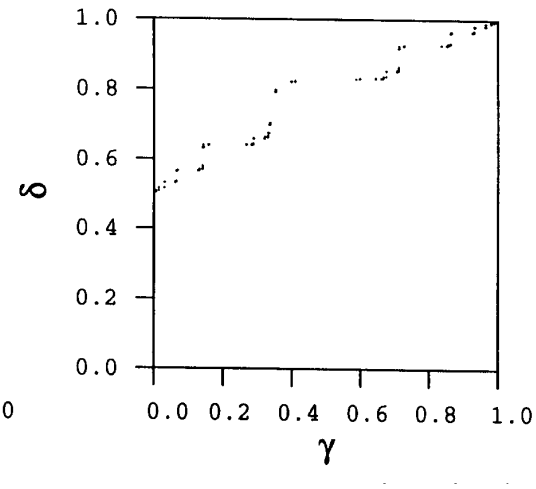

Figure 8.8: The pruning front for the wedge billiard for $\theta = 45.1°$.

which gives the symbolic values

$$\begin{aligned} \delta &= 0.10w_3w_4w_5\ldots \\ \gamma &= 0.0w_3w_4w_5\ldots \end{aligned}$$

From these equations we get (8.3). The other choice of $l_0'l_0$ gives the symmetric line $\gamma = \delta/2 + 1/2$.

Figure 8.5 shows the numerical pruning front obtained for the wedge billiard at 45° and figure 8.6 shows the symbolic values of a number of different (not chaotic) orbits in this wedge. Parameters close to 45° should give pruning fronts close to this straight line and in figures 8.7 and 8.8 we find for wedge angles $\theta = 45.01°$ and $\theta = 45.1°$ many points on the pruning front are close to the line $\delta = \gamma/2 + 1/2$ but some points are far above this line and gives a staircase like curve with the line as an envelope under the points.

8.2 4-disk

When the four disks are so close that the area of the domain where the particle bounces goes to 0 the walls of the domain approaches straight lines and the system becomes a particle in a square box. A particle bouncing inside a square is equivalent to a particle moving freely on a square lattice and again we get the symbolic description from the Farey tree construction. Here the translation from the rotation to the symbol plane is slightly more complicated because the alphabet in the 4-disk case is a four letter alphabet or a three letter alphabet.

We may choose to identify the four disk symbols $s_t \in \{1, 2, 3, 4\}$ with the lattice such that the symbols 1 and 3 correspond to horizontal lattice lines and the symbols 2 and 4 correspond to vertical lattice lines. Every second lattice line is then 1 and 3 (or 2 and 4) and every crossing of one of these lines gives these symbols alternating. We also immediately see that a clockwise bounce followed by a number of bounces between opposite disks gives a clockwise or anticlockwise bounce depending of whether the number of bounces was even or odd.

We can use the Farey tree in figure 8.3 to construct the symbolic strings for this system. As the well ordered symbols are of grater interest than the symbols s_t we only give the symbols w_t. Since the system is symmetric in the vertical and the

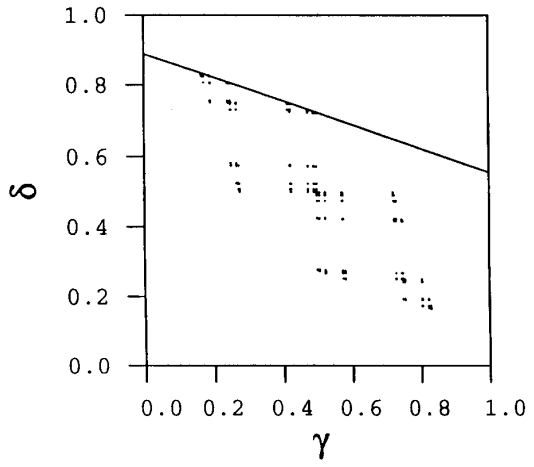

Figure 8.9: The symbolic values for a number of orbits in the overlapping 4-disk billiard close to the integrable limit with parameter $r = 1.416$ and the line $\delta = 8/9 - \gamma/3$.

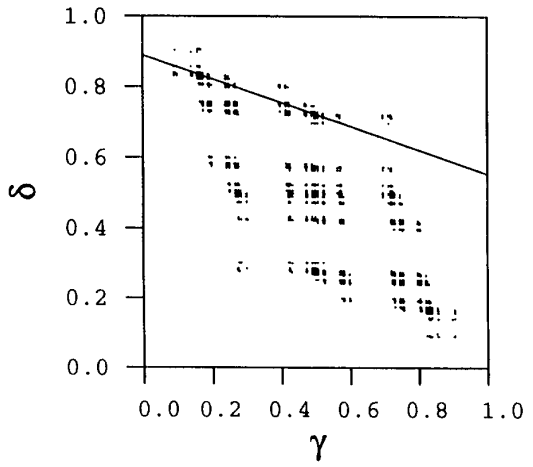

Figure 8.10: The symbolic values for a number of orbits in the overlapping 4-disk billiard with distance $r = 1.5$ between the disk centers and the line $\delta = 8/9 - \gamma/3$.

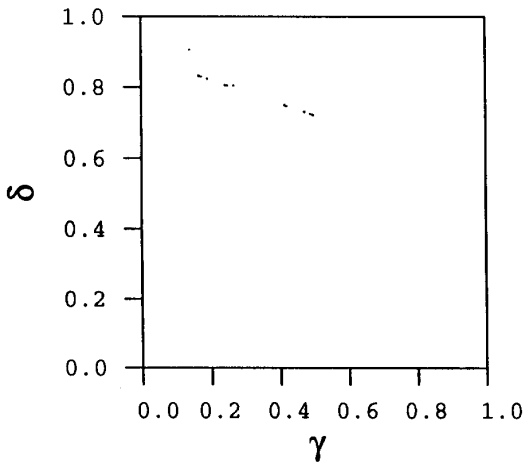

Figure 8.11: Corner pruning front for the overlapping four disk billiard close to the integrable limit with parameter $r = 1.416$.

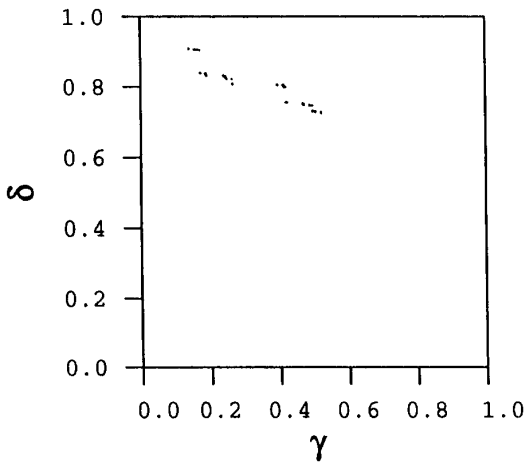

Figure 8.12: Corner pruning front for the overlapping four disk billiard with distance $r = 1.5$ between the disk centers.

horizontal direction we only have to use half the Farey tree to get w_t

$$
\begin{array}{lllll}
 & 20 & & & \\
 & & & 1202020 & 120202020 \\
 & & & & 120201202020 \\
 & & 12020 & & \\
 & & & 12012020 & 1201202012020 \\
 & & & & 12012012020 \\
 & 120 & & & \\
 & & & 1120120 & 1120120120 \\
 & & & & 11201120120 \\
 & & 1120 & & \\
 & & & 11120 & 111201120 \\
 & & & & 111120 \\
1 & & & &
\end{array}
\tag{8.4}
$$

In addition to these we have the strings where symbols 0 and 2 are interchanged.

The pruning front from the tangent orbits only becomes a point in these limit as there is no curvature left. As for the wedge the limit of the pruning front originating from the orbits starting in the corners is a straight line. Since the construction of well ordered symbols are different and have base 3 symbol values wee get a different line. Following an argument as above we find the line

$$\delta = \frac{8}{9} - \frac{1}{3}\gamma \tag{8.5}$$

to be the limit of the pruning front.

Figures 8.9 and 8.10 show the symbolic values of all bounces for chaotic orbits close to the limit $r = \sqrt{2} = 1.4142\ldots$. For the parameter $r = 1.416$ there is hardly any point above this line while for $r = 1.5$ there is some points above it. The figures 8.11 and 8.12 show the corner pruning fronts for the same parameter values. Close to the limiting parameter value the points of the pruning front are almost all very close to the line (8.5).

8.3 3-disk

In the limit when the three disks are so close that the domain turns into a triangle the orbit is equivalent to the straight line in a triangular lattice as showed in figure 8.2. The symbolic description of this can be found from the Farey tree in the following way; The line is always crossing in an angle between 60° and 120° to one of the three directions in the lattice. Every second crossing between the line and the lattice lines is a lattice line which has this direction. The non trivial dynamics is only the crossing between the line and the lattice lines in the other two directions. If we call the crossing of the line with a lattice line in one direction 0 and the crossing with a lattice line in the other direction 1 and skip the crossings

with the trivial lattice lines, then the Farey tree in figure 8.3 gives the grammar. There is no mathematical work on this triangular lattice proving that this is the correct procedure [192] but as it turns out to be very similar to the square lattice we state the result as a conjecture.

In figure 8.13 the triangular lattice is drawn and the labeling l_t is given as 1 for horizontal lines, 0 for lines going right-up and 2 for lines going right-down. In the lattice we have drawn a line going from left-down to right-up. This line crosses the lattice lines no 2 every second time it crosses a lattice line and analogous to the square lattice we can construct the Farey tree with these lattice line symbols l_t assuming every second crossing is 2. This gives the following tree for l_t

$$
\begin{array}{llll}
21 & & & \\
 & & 20212121 & 2021212121 \\
 & 202121 & & 20212120212121 \\
 & & 2021202121 & 2021202121202121 \\
2021 & & & 20212021202121 \\
 & & 2020212021 & 20202120212021 \\
 & 202021 & & 2020212020212021 \\
 & & 20202021 & 20202021202021 \\
20 & & & 2020202021
\end{array}
\tag{8.6}
$$

The orbit in figure 8.13 has the labeling in symbols $l_t \ldots 2120212120 \ldots$ and we find that this is a substring of the string 2021202121202121 in the Farey tree (8.6).

The three symbols s_t in the 3-disk system are not identical with the three directions of the lattice lines, but the disk symbols can be identified with the parts of the lattice lines as showed in figure 8.14. This unfolding of the domain to the lattice gives the new symbols and we obtain a Farey tree for the symbol s_t which is rather awkward to use because the symbols are not repeated the same way. Assuming we first cross the line with symbol 2 as in the figures we obtain the tree for s_t

$$
\begin{array}{llll}
21 & & & \\
 & & 23132132 & 2313213213 \\
 & 231321 & & 23132131213213 \\
 & & 2313231321 & 2313231321312132 \\
2313 & & & 23132313231321 \\
 & & 2312321232 & 23123212321232 \\
 & 231232 & & 2312321231213121 \\
 & & 23123121 & 23123121312313 \\
23 & & & 2312312313
\end{array}
\tag{8.7}
$$

It is simpler to directly work with the well ordered symbols w_t. In this alphabet

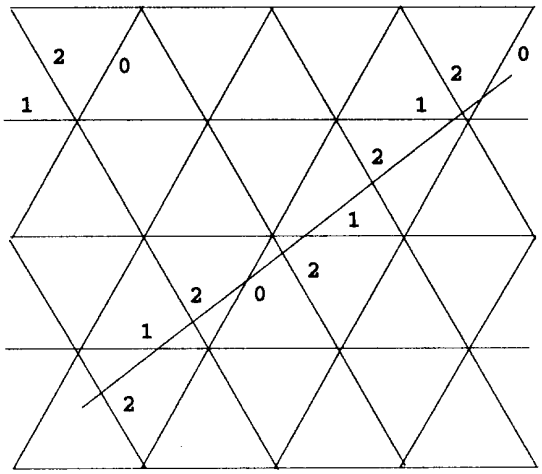

Figure 8.13: The triangular lattice with a symbol l_t for each direction and a line giving the sequence $\ldots 2120212120 \ldots$.

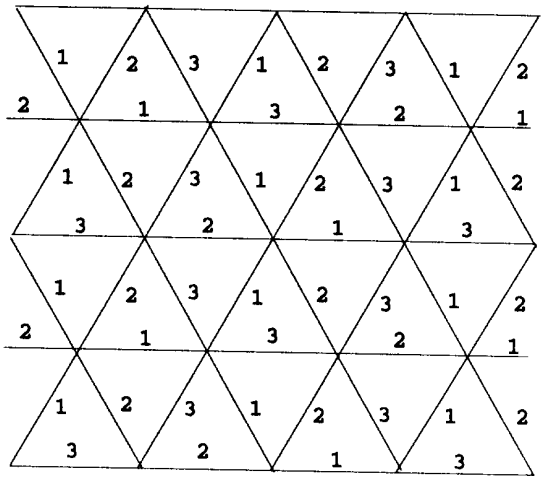

Figure 8.14: The triangular lattice with the symbols s_t for the 3-disk system folded out in the lattice.

we obtain the tree for symbols w_t

$$
\begin{array}{lllll}
10 & & & & \\
 & & & 01101010 & 0110101010 \\
 & & & & 01101001101010 \\
 & & 011010 & & \\
 & & & 0110011010 & 0110011010011010 \\
 & & & & 01100110011010 \\
 & 0110 & & & \\
 & & & 0101100110 & 01011001100110 \\
 & & & & 0101100101100110 \\
 & & 010110 & & \\
 & & & 01010110 & 01010110010110 \\
 & & & & 0101010110 \\
01 & & & &
\end{array}
\tag{8.8}
$$

We can get the limit of the corner pruning front by observing the well ordered symbols w_t for a line going through a lattice cross. We choose the symbols for going through the cross as three symbols for crossing close to the cross and obtain

$$
\begin{aligned}
\gamma &= .0w_2w_3w_4\ldots \\
\delta &= .110(1-w_2)(1-w_3)(1-w_4)\ldots
\end{aligned}
$$

which gives the line

$$\gamma = \frac{7}{8} - \frac{1}{4}\delta \tag{8.9}$$

In figure 8.15 this line is plotted together with a number of bounces in the 3-disk billiard for the center-center distance $r = 1.7325$ which is close to the critical

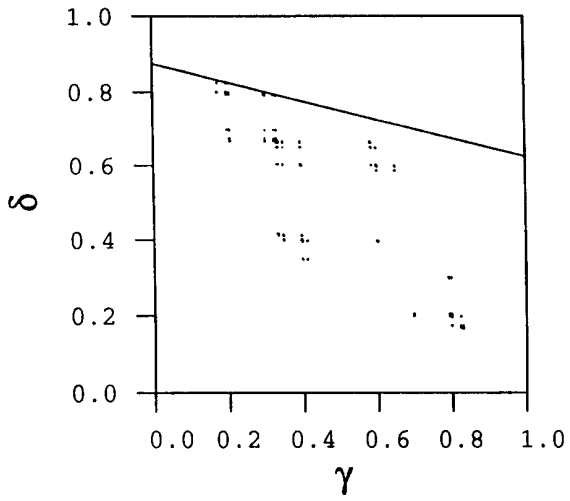

Figure 8.15: The symbolic values for a number of orbits in the overlapping 3-disk billiard close to the integrable limit with parameter $r = 1.7325$ and the line $\delta = 7/8 - \gamma/4$.

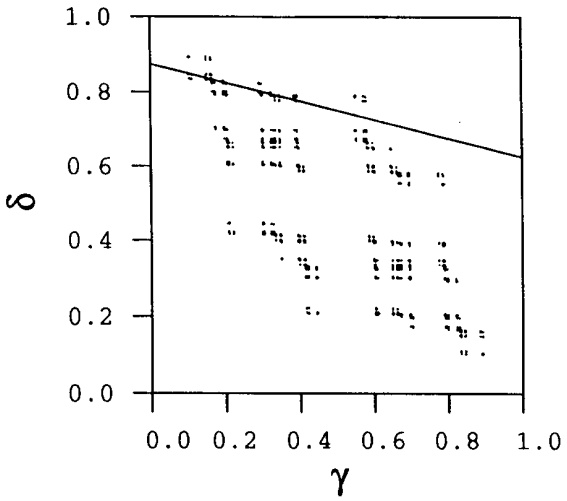

Figure 8.16: The symbolic values for a number of orbits in the overlapping 3-disk billiard with distance $r = 1.738$ between the disk centers and the line $\delta = 7/8 - \gamma/4$.

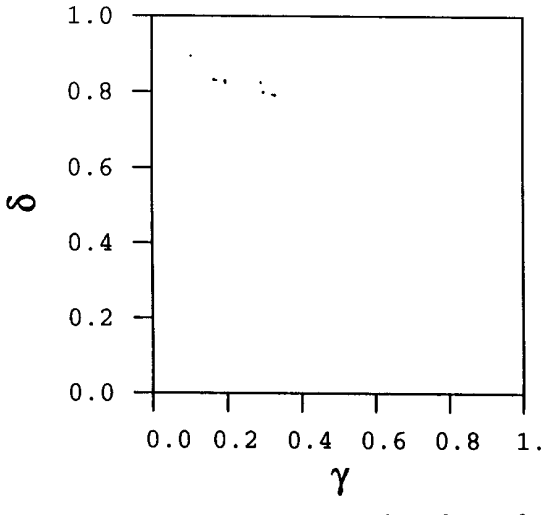

Figure 8.17: Corner pruning front for the overlapping 3-disk billiard close to the integrable limit with parameter $r = 1.7325$.

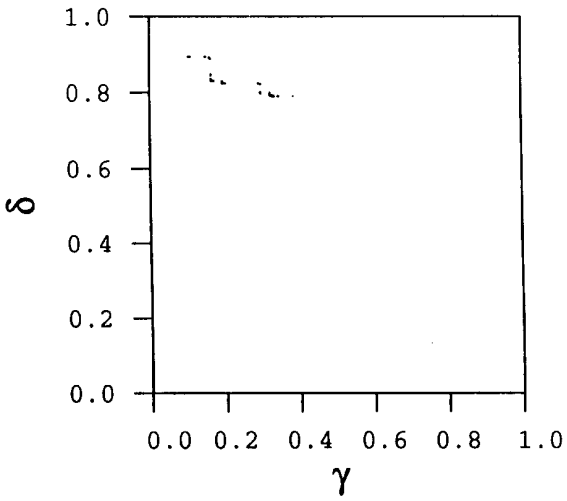

Figure 8.18: Corner pruning front for the overlapping 3-disk billiard with distance $r = 1.738$ between the disk centers.

distance $r = \sqrt{3} = 1.73205\ldots$. In this numerical experiment we do not get any points above the line. A slightly larger parameter value $r = 1.738$ gives figure 8.16 where a few of the points are above the line. The corner pruning fronts for these two parameter values are drawn in figures 8.17 and 8.18. The pruning front becomes points on the line (8.9) in the limit $r \to \sqrt{3}$.

8.4 Approaching the integrable limit from the mixed chaos-order side

The limit of orbits organized in a Farey tree gives a signature which is a pruning front that becomes a straight line. In a phase space plot of a chaotic orbit there is no clear signature of this organization.

We can however in these cases approach the integrable limit tuning the parameter from the opposite side of the critical parameter value. We then have a system with mixed chaos and stable islands. This is the dynamics for the wedge billiard (the two ball system) for $\theta < 45°$ ($m_1 < m_2$) and for the disc systems where the walls are slightly convex instead of concave. We can to study a disc system as a particle bouncing inside the convex domain limited by the focusing side of the disk walls for the 3-disk system with center-center distance less than $\sqrt{3}$.

The dynamics we observe in the wedge billiard and in the 3 disk system is that all stable islands close to the limit of the critical parameter value are islands surrounding each periodic orbit from the Farey tree construction. Approaching the limit, the islands become squeezed out into horizontal lines in the phase space. In the integrable system the orbits are degenerated and are lines instead of points in the phase space.

Pictures of the island structure for the wedge billiard was drawn by Lehtihet and Miller [131] and discussed in several articles [167, 197]. In figure 6.9 b) we find that in the limit $\theta \to 45°$ there is a hierarchy of islands with an island surrounding each periodic orbit from the Farey tree (8.1). For a θ finitely smaller than 45°, the smallest islands have disappeared in a chaotic sea. In smooth dynamical systems like the standard map [134], the KAM theory gives that quasiperiodic orbits with irrational winding number survive a perturbation depending on how irrational they are in a Farey tree sense. The Last surviving KAM tory has the golden mean as winding number. In these billiard systems it seems that the creation of chaotic regions also follows a Farey organization but here we do not have the unstable periodic orbit which give the chaotic regions and the mechanism of creating chaos is different. It seems that the stable periodic orbits furthest down in the Farey

tree disappear and create a chaotic region first. This imply that the orbits with most irrational winding numbers first disappear in the chaotic sea. This is in a way opposite to the KAM-scenario. The numerics indicate that the transition to chaos is different in these discontinuous systems than in the smooth flows and maps.

As the value of the parameter θ in the wedge billiard decreases the system "forgets" the Farey tree organization, and in the limit of a very narrow wedge $\theta \to 0$ the dynamics is dominated by one stable orbit.

We may compare the wedge billiard scenario with a disk system to examine how general the wedge billiard transition from integrability is. We know that the dispersive 3 disc billiard is completely chaotic and in the integrable limit it has the orbits organized in a Farey tree. The phase space picture of a number of different orbits in the focusing 3-disk system is plotted in figure 8.19 for different parameter values from close to the triangle shape, $r = \sqrt{3}$, to almost a circle, $r = 1$. In figure 8.19 a) there are islands which are very narrow and hard to distinguish but in figure 8.19 b) it is possible to distinguish a number of islands which surrounds the shortest of the periodic orbits from the Farey tree. When r decreases as for figure 8.19 c) we find that only the largest of the islands in figure 8.19 b) remain. As the value of r decreases further we find that the picture changes into new structures and only the stable period 3 orbit $\overline{s_1 s_2 s_3} = \overline{123}$ survive to $r \to 0$ and is here dominating the dynamics. This dynamics is qualitatively similar to the wedge for $\theta \to 0^\circ$ where the orbit bouncing back and fort between the two tilted walls dominates and to the two ball system where the dominating orbit for $m_1 << m_2$ is when the down-most ball bounces off the floor and bounces in the upper most ball every time.

We have not proven that the islands in figure 8.19 are surrounding the periodic orbits of the Farey tree, but this seems to be a reasonable conjecture from the numerical pictures. The different examples suggest that there is a number of systems that have this kind of transition to chaos, and this may be generic for non-smooth billiards.

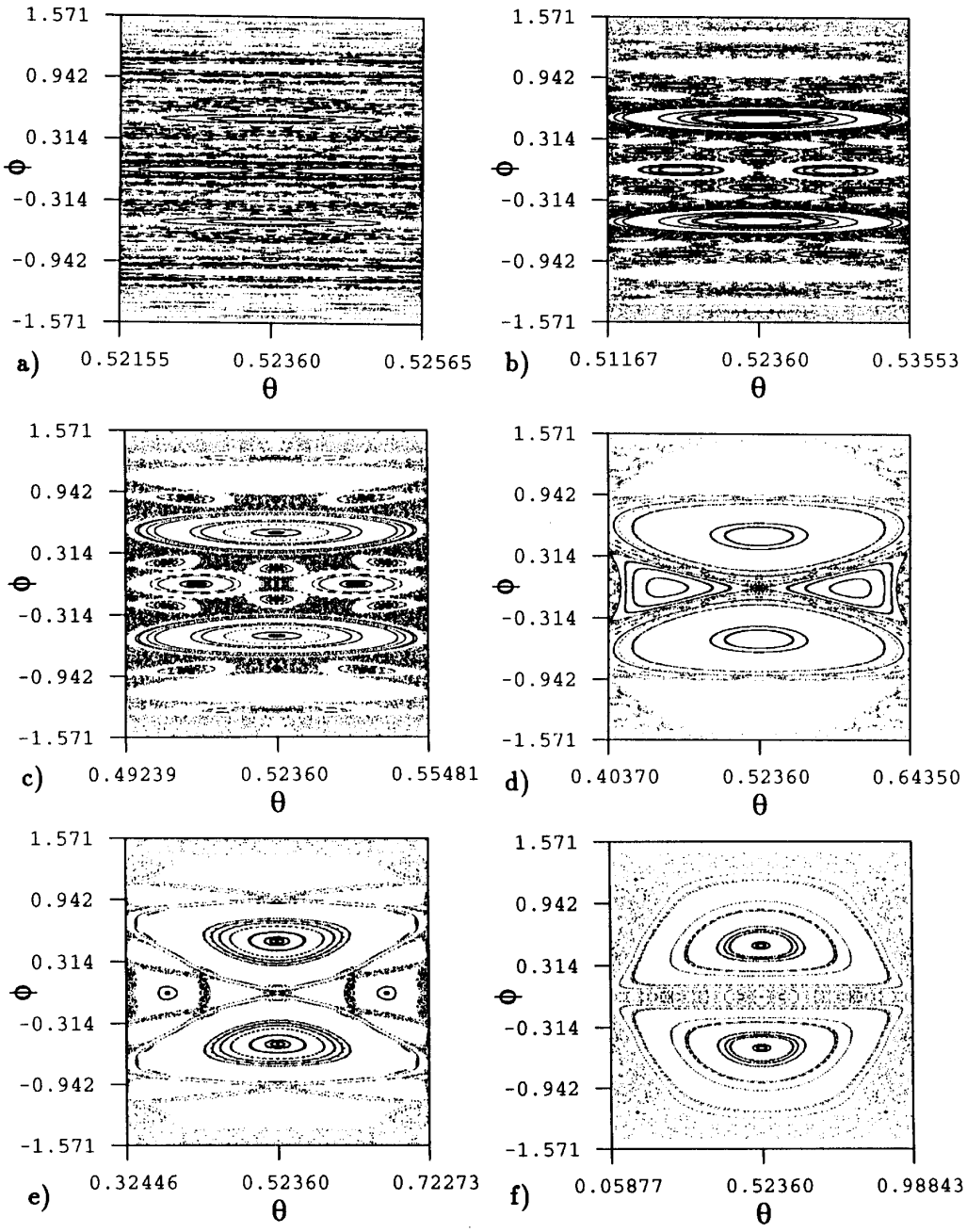

Figure 8.19: The phase space plot of orbits in the mixed stable-chaos 3 disk system. a) $r = 1.73$, b) $r = 1.72$, c) $r = 1.7$, d) $r = 1.6$, e) $r = 1.5$, f) $r = 1.1$,